Propagative Paper

Sustainable Seismic Design Guidelines of Steel Earthquake Resisting Structures

Razie Ansari Targhi[1], Marzie Ansari Targhi[2*], Mark Grigorian[3] and Vahid Broujerdian[4]

1. Ph.D. Candidate, School of Civil Engineering, Iran University of Science and Technology, Tehran, Iran
1. Ph.D. Candidate, Faculty of Civil, Water and Environmental Engineering, Shahid Beheshti University, Tehran, Iran,
*Corresponding Author; email: m_ansaritarghi@sbu.ac.ir
3. D.Phil., MGA Structural Engineering Consultant Inc,Glendale, California, USA
4. Associate Professor of Civil Engineering, Iran University of Science and Technology, Tehran, Iran

Received: 31/07/2024
Revised: 04/09/2024
Accepted: 16/09/2024

ABSTRACT

Recently, a number of much-needed innovations have captured the attention of the earthquake engineering communities worldwide: the stiff braced rocking core, as part of conventional steel earthquake-resisting systems (ERS); the introduction of low-damage systems and components; the use of triple and mixed multiple seismic structures; and the sustainable seismic design (SSD) philosophy with a view to economy and environmental protection. SSD has been the most challenging issue confronting structural engineers for decades. Regardless of carbon footprint reductions, unless a structure is designed for seismic sustainability, it would be disposable with greater human discomfort, economic loss, and harm to the environment. In the present context, design implies planning for controlled seismic resistance, environmental protection, construction economy and Post-earthquake Realignment and Repairs (PERR). In SSD, the practicality of PERR is as important as the relevance of the theoretical assumptions; therefore, the non-lateral resisting items are carefully designed not to partake in seismic resistance. All Earthquake Resisting Structures (ERS) are designed for practical, residue-free recentering while their energy-dissipating components are detailed to remain repairable/replaceable after the event. In the interim, new categories of ERS and innovative ideas have also been introduced. The authors hope this and related articles will form the basis of SSD guidelines for earthquake-prone resilient cities.

Keywords:
Rocking cores; Mixed multiple, Sustainability; Energy dissipation; Collapse prevention; Recentering

How to cite the article:
Ansari Targhi, R. , Ansari Targhi, M. , Grigorian, M. & Broujerdian, V. (2025). Sustainable Seismic Design Guidelines of Steel Earthquake Resisting Structures. *Journal of Seismology and Earthquake Engineering*, *27*(2), 45-64. doi: 10.48303/jsee.2024.2037265.1116

1. Introduction

SSD is a new doctrine that promises the economy, real-time seismic safety, and environmental protection for earthquake-prone regions of the world. In the present context, seismic sustainability for engineering structures implies enduring limit state conditions through severe earthquakes without loss of life and catastrophic collapse. The advents of the stiff spine, MacRae et al. (2004), Mahin (2017), Akbari et al. (2023), the low-damage energy-dissipating fuses, Ma et al. (2011), Grigorian and Grigorian (2017), and rigid rocking cores, Wada et al. (2012), Grigorian and Grigorian (2015), Fahnestock et al. (2021) have been highly instrumental in developing the SSD doctrine. Here, the economy is attributed, in the first place, to "Plastic design" principles, Beedle (1985), Heyman (1971) and the "Uniqueness theorem", Neal (1963), that axiomatically result in minimum weight solutions for low damage ERSs, Foulkes (1953), Brandt (1978). Secondly, it is always more cost-effective and less burdensome to repair a low damage structure than build anew. Lastly, the downtime for financial losses due to earthquakes are considerably reduced, IACGE (2018), Wang & Hua, (2018), Grigorian et al. (2023), Ansari et al. (2024). There are no physical mechanisms to ensure "Life-safety" and "Collapse prevention" as referred to in contemporary codes of practice, e.g., Eurocode-8 (1998), ASCE/SEI 7-16 (2016). SSD depends on the provision of physical restraints to prevent actual collapse and avert damage beyond repair. Currently, SSD is neither part of contemporary design guidelines nor collage curricula, Wada and Mori (2008), Takagi and Wada (2019). There are three methods of approach for SSD: (a) the conventional methodologies, which advocate maintaining a completely elastic response throughout the loading history of the structure, as described in most pre-northbridge and some current codes of practice, e.g. (UBC, 1992), (b) the classic approach, which also advocates maintaining linear response during earthquakes by means of active and/or passive controls, as discussed by Karavasilis et al. (2011), Lu and Panagiotou (2014), Naiem (2001), Spencer and Nagarajaiah (2003) and Yao (1972), and (c) the contemporary methods that rely on the ductility of ERS and the recentering capabilities of built-in or auxiliary systems, as reported by, among others, Hajjar et al. (2013), Wiebe and Christopoulos (2014), Chancellor et al. (2014), Bozkurt and Topkaya (2018), who have focused attention on theoretical as well as experimental aspects of free-standing, self-aligning RRCs with and without energy dissipating devices. It has also been demonstrated by Ajrab et al. (2004), Grigorian and Kamizi (2019a), Janhunen et al. (2012), Pollino et al. (2017) that RRCs can enhance the seismic response of conventional steel ERS, prevent collapse, and sustain repairable damage. The difference between these methodologies is not only in the ways they address seismic response but also in the behavior of the system after the event. SSD is a multifaceted undertaking that involves both natural as well as manual modes of action (Gilmore, 2012; Pessiki, 2017), Earthquakes are short time, natural and dynamic events, whereas PERR are time-consuming, manual, and static operations. In SSD, resolution of over-simplified assumptions and mitigation of conflicting structural actions is as important as assuring robust, natural seismic response of the system. For instance, gravity members and nonstructural items not designed for seismic loading may partake in resisting earthquakes but oppose the realignment process. Henceforth, it would be detrimental to SSD not to isolate the elements of the gravity structure and architectural features for seismic conditions, as they may be damaged beyond repairs due to large distortions and accumulation of residual effects. The P-delta effects magnify the seismic demand and hinder the PERR effort. SSD involves purpose-specific computations, detailing, as well as planning for "Performance control" (Priestley & Kowalsky, 2000; Grigorian & Grigorian, 2011, 2012), collapse prevention (CP), Fail safe (FS) technologies, and PERR. FS mechanisms are meant to reduce and/or prevent larger-than-expected displacements due to the formation of failure patterns within the ERS and to activate the post-yield reserve capacities of the structure for CP and PERR. Consequently, the development of SSD entails combinations of different methods of approach, including recognition and improvement of inadequate design concepts, use of adaptive technologies, and comparative functional analysis. The focus of the current article is on SSD of dual ERS. The role of the RRC, as an indispensable component of the proposed system, is briefly discussed in the forthcoming sections of the paper.

2. Development of the First-Generation SSD Principles

Despite significant advances in the fields of structural analysis, modeling, and energy-dissipating devices, the importance of SSD has not been fully recognized by governing authorities worldwide. There are several reasons for the slow-paced progress in this field, most significantly, poorly defined basic design concepts, over-simplified computational assumptions, and the use of unfavorable or purpose-defying details. Amongst myriads of code-sanctioned ERSs the dual steel moment frame-shear wall/RRCs are best suited for SSD upgrading. Dual ERSs are potentially capable of allowing one of the two structures, preferably the ductile system, to form a failure mechanism without falling apart, while the other prevents collapse and harvests seismic energies for PERR purposes. In practice, several ERSs can be combined to achieve SSD. Many of the pioneering innovations in this field, such as the continuous stiff column/the rigid spine and energy harvesting systems (Eatherton et al., 2014; Pampanin, 2015; Grigorian et al., 2020) that were used to develop early seismic sustainability archetypes, are still unknown in most earthquake-active regions of the world. The proposed first-generation SSD details, may not be perfect but are better suited for SSD of steel SSD framing than their traditional counterparts and pave the way for further improvements in the future. In this section, resort has been made to comparative functional analysis to upgrade conventional seismic design of steel dual shear wall combinations to SSD within the realms of current engineering practices. The classical "Pushover" curve, Figure (1a) symbolizes the basic concepts involved in the design of conventional, ductile ERSs. However, it does not address the multi-functional conditions of SSD. The plot neither indicates the possibility of recentering nor the use of restoring systems, as depicted in Figure (1c). It does not reflect loss of stiffness caused by the P-delta effects, as shown in Figure (1b), nor gain of strength due to strain hardening. Thus, there is a reason to upgrade the applications of the pushover plot to a complete response diagram, including the effects of both restoring and disruptive forces, so that the inner workings of SSD may be closely studied. Points a and b of Figure (1a) signal specific states of response, whereas point c relates to an obscure endpoint for the event, it may at best refer to permanent deformation of the system with locked-in permanent residual stresses. In these plots, ϕ_y, ϕ_{FS} and $\phi_{\max}$ at point c represent yield, fail-safe and maximum drift ratios, respectively. Distances *oc* and *bc* imply the existence of a large residual deformation and a residual force equal to that of the earthquake respectively, conditions that are neither feasible nor desirable. The form of the basic plot can be improved by including the unloading path, line *bf* , in the half-cycle hysteresis diagram of Figure (1d), which in the absence of a return cycle, such as segment *fgh* of Figure (1e) hints at the possibility of post-

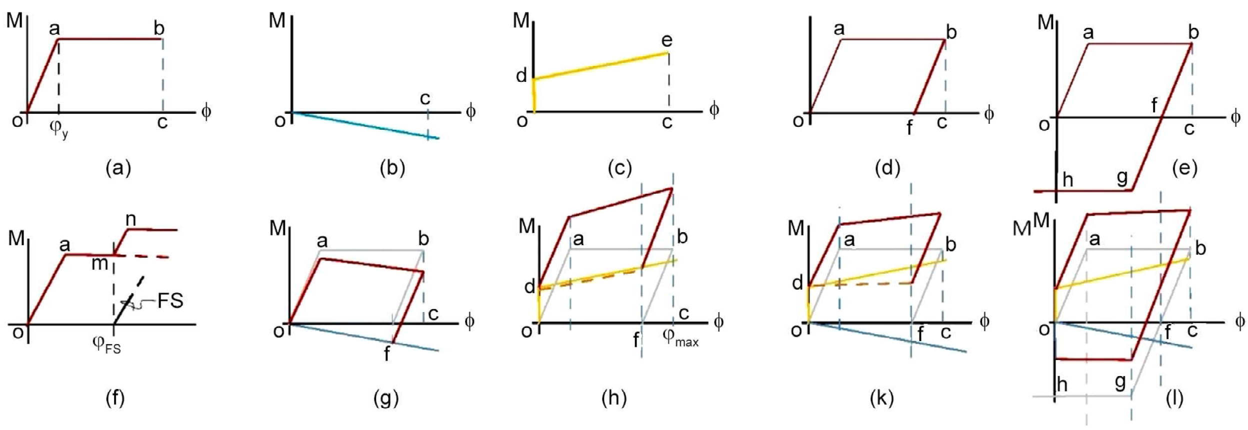

Figure 1. (a) Standard pushover plot, (b) Phantom P-delta plot, (c) Restoring force with preloading, (d) Pushover + unloading, (e) Pushover + reloading+ recentering, (f) Pushover +Fail-safe, (g) Pushover +unloading+ P-delta, (h) Pushover +unloading+ restoring force, (k) Pushover +unloading +P-delta + restoring force, (l) Recentering Pushover +unloading+ reloading +P-delta +restoring.

earthquake manual realignment along line *fo*. Point o of Figure (1d) indicates ideal, residue-free realignment. Figure (1e) presents a full-cycle response of the structure and the termination of automatic or forced realignment accompanied with a large residual force, *oh*, equal to that of the earthquake. Figures (1g) and (1h) show the effects of the P-delta and the restoring forces on the response of the original ERS, respectively. These effects tend to reduce and increase the carrying capacity of the system. Figure (1f) reflects the possibility of increased strength due to strain hardening or mechanical intervention. This observation is the basis of the FS concept introduced in Section 3 below. Activation of the FS device before or at ϕ_{FS} or $\phi_{\max}$ can delay and prevent catastrophic failure in the absence of other CP systems. Figures (1k) and (1l) depict the combinations of the half-cycle and full-cycle plots with P-delta and restoring effects, respectively. A comparison of these two plots suggests that the realignment effort can be minimized by reducing the post-earthquake stiffness of the system and replacement of the damaged parts. Figure (1k) also hints at the possibility of overcom-ing the residual forces by selecting the preloading force $od \geq oh$. These observations form the basis of the "Global Stiffness Reduction" (GSR) and Restoring Force Adjustment (RFA) technologies introduced in the forthcoming sections of this article. The full-cycle diagrams also indicate four distinct stages of response associated with SSD, namely: 1- the at-rest or normal service stage (static conditions), 2- during strong ground action (dynamic conditions), 3- the post-earthquake hiatus (static conditions), and 4- Recentering and repairs (static conditions).

Since the multistate conditions of seismic sustainability structures and predefined locations of controlled damaged parts are known, the entire system lends itself well to health monitoring, manual control and adjustments (Grigorian et al., 2022). What plots (a) and (f) do not show is what can happen after the event and before PERR is completed. Nevertheless, it is prudent to consider the possibilities of aftershocks, disruption of life-lines, and collapse of non-structural components that can be isolated by proper detailing. The next section examines the use of independent structural systems that closely follow the response paths of Figure (1k). These systems include, but are not limited to:

- Gravity and architectural systems that neither partake in seismic resistance nor hinder the realignment process, e.g., simple, highly articulated, steel, beam-column joints (Figure 2a),
- ERS composed of low-damage beams, columns, braces, and accessible, replaceable energy-absorbing fuses, e.g., purpose-specific steel moment frames (MF) and/or EBFs (Figures 3b and 3c),
- Collapse-preventive systems with or without FS devices, e.g., rigid rocking cores (Figure 4e),
- Adjustable realignment devices e.g., post-tensioned tendons equipped with stressing devices,
- Low-damage column base supports, such as continuous grade beams (Figure 2c),
- Supplementary systems such as active/passive control and other energy dissipating devices.

2.1. Development of the SSD Details and Connections

Almost all codes of practice advocate idealized performance-based designs and theoretical CP for maximum considered earthquakes. Low-damage, repairable/replaceable designs are not mentioned in contemporary design guidelines. However, since the envisaged performance criteria are not in congruity with the self-operating systems of as-built structures, they may not collapse due to strong ground motion but will deform beyond repairs and become disposable (Kam & Jury, 2015; Grigorian et al., 2019b). SSD is a concept that requires a thorough understanding of the mechanics of residual stresses and strains, energy control, physical CP, and PERR. The multi-stage nature of seismic sustainability operations-during at rest and PERR-calls for a transition from well-established classical methodologies, as in performance-based design (Gunay & Mosalam, 2013) to nature-oriented design and similar philosophies (Grigorian, 2014a, 2014b; Grigorian & Kamizi, 2019c). The use of purpose-specific details leads to the development of economically feasible archetypes that rely upon commercially available materials, technologies, and conventional methods of construction. Having established Figure (1k) as the full-cycle response plot of a single-degree-of-freedom system with potential recentering characteristics, it remains to develop the details of the corresponding parts and joints needed to assemble an economical seismic sustainability archetype.

There are two conditions where near-perfect, post-earthquake realignment can take place: (1) If the entire building system remains totally elastic after the event, and (2) when all non-earthquake-resisting components are either seismically detached or can be isolated from the reparable ERS. All gravity structures and architectural appendages tend to resist earthquake forces in proportion to their neglected stiffnesses and hinder the re-centering process due to earthquake-induced permanent deformations. Simplifying assumptions that favor theoretical expediency and ease of construction tend to hinder the PERR process. Consequently, no conventional system can become seismically sustainable unless its details and connections are modified specifically for the purpose. An assessment of the suitability of standard steel details reveals that the so-called "simple or hinged joints" for gravity framing, e.g., Figure (2d), should be replaced with articulated connections such as those shown in Figures (2a) and (2b), respectively. Over-restrained, simple connections, such as Figure (2d) are potentially prone to absorbing residual effects due to large seismic displacements (Richards et al., 1980; Astaneh Asl et al., 1989). The radially placed elongated holes on the web plate of Figure (2a) allow the transmission of axial and shear forces without resisting moments. The horizontally elongated holes of the angle cleats to column connections reduce beam torsional moments on the column. Figure (2c) proposes a conceptual moment-free base support for steel columns.

2.1.1. The Column Support-Grade Beam Arrangement

An important issue often overlooked in contemprary literature on self-centering, rocking cores, and low-damage systems, is the effects of large seismic displacements on column support conditions. Almost all reinforced concrete colums and steel stanchions, especially those marked for seismic resistance, are fully fixed at their supports. Damaged footings and column supports are most difficult to repair, to the extent that the entire structure may become unusable. Such damage can be alleviated by replacing fully fixed column supports with totally articulated joints and energy-absorbing grade beams such as those shown in Figure (2c). Intelligently designed grade beam systems can also prevent grade level soft-story failure and help maintain uniform drift along the height of the structure.

2.1.2. The Seismic Sustainability Beam-Column Details

The purpose of this section is to introduce a practical design concept for steel, seismic-

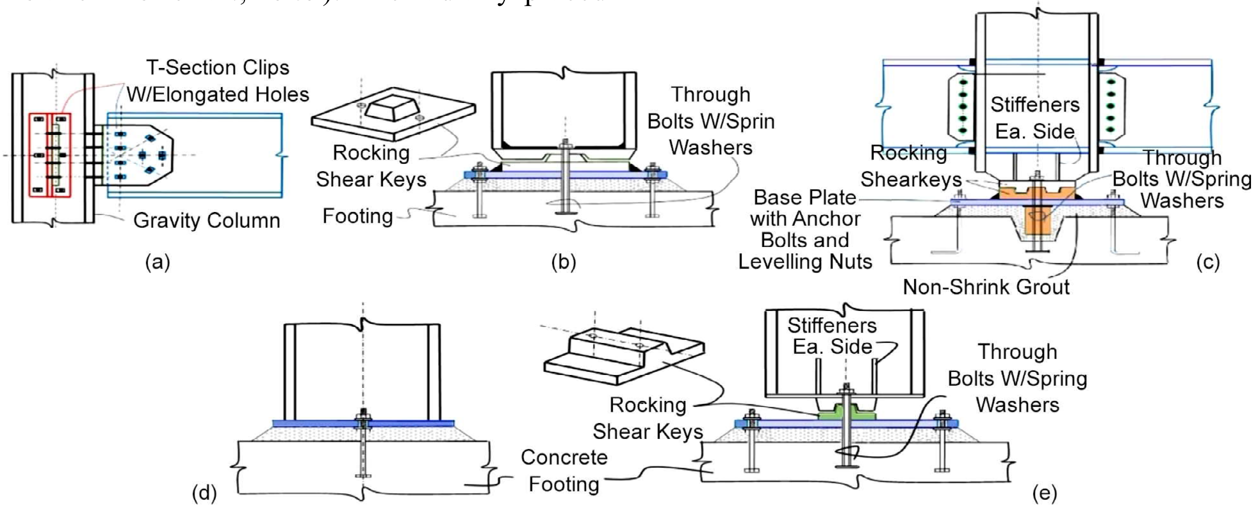

Figure 2. (a) Proposed articulated beam-column joint with torsion release, (b) Proposed two-way rocking pinned base column support, (c) Proposed rocking base column support, partial fixity provided by grade beams, (d) Typical pinned column base and (e) Proposed one-way rocking pinned column support.

sustainability, minimal damage MFs with self-aligning beams and replaceable joints that can dissipate large amounts of seismic energy. The proposed arrangement is a modification of the steel column-tree MF shown in Figure (3a) by Astaneh (1997). Properly designed column-tree assemblies are ideally suited for erecting steel MFs. They tend to develop plastic hinges within the end stubs without damaging the adjoining columns. Standard column-trees are neither capable of realignment nor preventing seismic damage to the bolted joints and the body of the beam.

To fix the locations of the plastic hinges away from the faces of the columns, the newer versions of column-tree assemblies, e.g., Figure (3a), are treated with reduced beam sections (RBS) on the top and bottom flanges of the beam. However, the RBS treatment does not prevent damage to the beam and the bolted joints, and as such, the assembly may become irreparable. Moreover, regardless of the desirable performance of the RBS systems, the formation of plastic hinges at column supports renders the entire MF incapacitated. The proposed layout becomes even more attractive if practical repairs following realignment is envisaged. The complete scheme of one such beam is suggested in Figure (3b). The proposed arrangement consists of the following components:

1. A three-piece compact steel wide-flange section or equal with prequalified stub-column connections,
2. Purposely detailed, moment-released shear plates connecting the three pieces to each other,
3. Replaceable, bolted, reduced-section, energy-dissipating top and bottom flange plates as shown,
4. Optional, replaceable, bolted, fail-safe top and bottom flange plates as shown,
5. Optional, crisscrossing, slightly tensioned high-strength tendons for realignment purposes, and
6. Optional pairs of permanent turnbuckles for recentering and fail-safe purposes.

The crisscrossing tendons are meant to counter

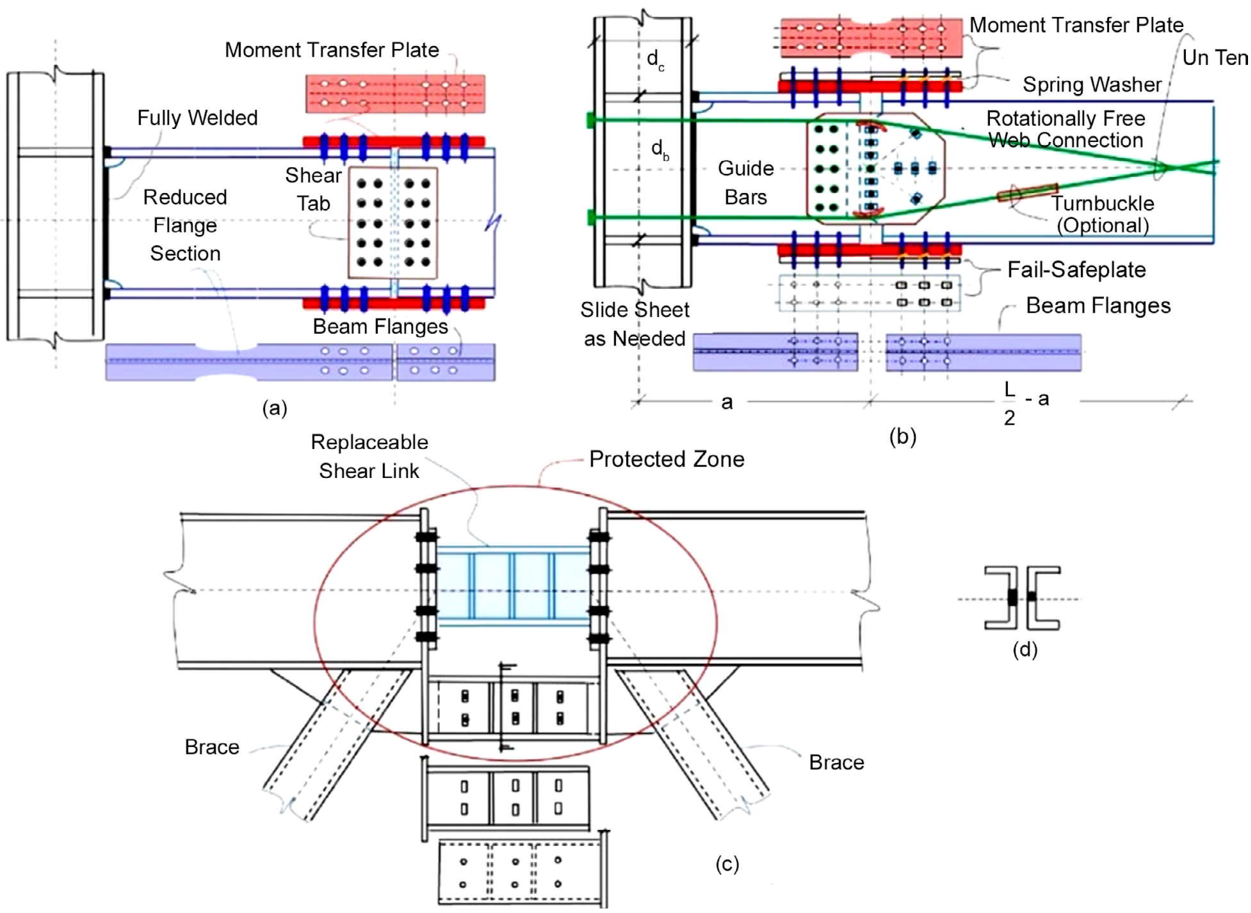

Figure 3. (a) Original column-tree joint, (b) Multi - purpose joint with FS plates, restoring tendons and turnbuckles, (c) Proposed replaceable shear link and FS device for EBF, and (d) Section through FS device.

gap openings on opposite flanges of the beam, whereas parallel tendons defeat the purpose by canceling equal gap opening and closing of the joints of the same flange.

Dowden and Bruneau (2011) have shown that conventional gap-opening steel beams with parallel tendon profiles tend to result in harmful and often destructive "frame expansion" due to "beam growth" during lateral movement. The proposed earthquake-resisting steel beam system, equipped with replaceable energy dissipating moment connections and nonparallel tendon profiles (Figure 3b), not only avoids "frame expansion", controls seismic response, and limits material damage, but also lends itself well to PERR activities. The optional tendons can be utilized either on their own as fail-safe and recentering devices or in conjunction with RRCs and other supplementary systems. The web-to-web connections have been detailed to avoid moments and accumulation of residual effects, and to facilitate the recentering process. The entire beam section and joints, except the FS and cover plates, are designed to remain elastic throughout the loading history of the MF. All joints are protected zones.

3. Physical Collapse Prevention; Means and Methods

PERR is achievable after ensuring physical CP and keeping the system stable as needed. Here, the often-neglected natural feature of ductile ERS, the post-yield capacity, is imitated to devise a new mode of activating the reserve strength of the structure. The use of FS systems, such as the compression sleeves of Figure (Appendix c), the strategically placed high-strength cables and/or large displacement inhibiting devices, shown in Figures (3b) and (3d), can help achieve collapse prevention. The FS plates are temporarily reinstalled one at a time after both FS and flange plates are removed for PERR. In fact, as the earthquake subsides, the P-delta effect continues to push the structure towards collapse. The P-delta moment diminishes as the structure is returned to its original position.

RBS joints tend to reduce the global capacity of the ERS in favor of damage control but do not effectively reduce the global stiffness of the structure. Numerical case studies show that RBS treatment can reduce the strength of the MF by as much as 30% of the strength of the beams. FS systems also compensate the reduced capacity of the beams and stabilize the system during the restoration processes. Note that activation of the FS plates shifts the natural plateau of Figure (1f) from point *m* to point *n*. Conventional ERS and their parts are designed for service and seismic conditions, with no guarantees against collapse. In multi-function design, the same members are detailed for several, sometimes opposing scenarios, with a view to continued service under all conditions. FS-enhanced joints control seismic response and help prevent physical collapse during and after the event. Removal of the damaged flange plates reduces the post-earthquake stiffness of the structure and facilitates the PERR effort. FS devices can be used advantageously to stabilize the unstiffened structure until the new flange plates are installed. The differences between the conventional and proposed connections are clearly illustrated in Figure (3). The response of the FS plates is characterized by their activation displacement ϕ_{FS} and plate strength (Figure 1f).

4. The Seismic Sustainability Dual Multi-Purpose MF-Hybrid RRC Scheme

The components and details proposed for the seismic sustainability dual system can now be assembled as presented in Figure (4), where the articulated gravity structure, the multi-purpose MF and the stabilized RRC are connected to each other in parallel through axially rigid, pin-ended, imaginary link beams. Figure (4f) portrays the individual response diagrams of the RRC, MF, FS and the phantom P-delta system, where M_R stands for moment of resistance. Let M_F, M_C, M_o, K_F, K_C and K_s stand for the external moments and stiffnesses of the MF, the stabilized RRC and the combined system, respectively. Similarly let $M_{(P\delta,F)}$, $M_{(P\delta,C)}$. $M_{P\delta}$ and M_F^P, M_C^P, and M_P define the P-delta and plastic moments of resistance of the MF, the RRC and the dual structure, respectively. Therefore, the ultimate capacity of the combined structure can be computed as the sum of the capacities of the two elastoplastic systems, i.e., $M^P = M_F^P + M_C^P$ and that the stiffness of

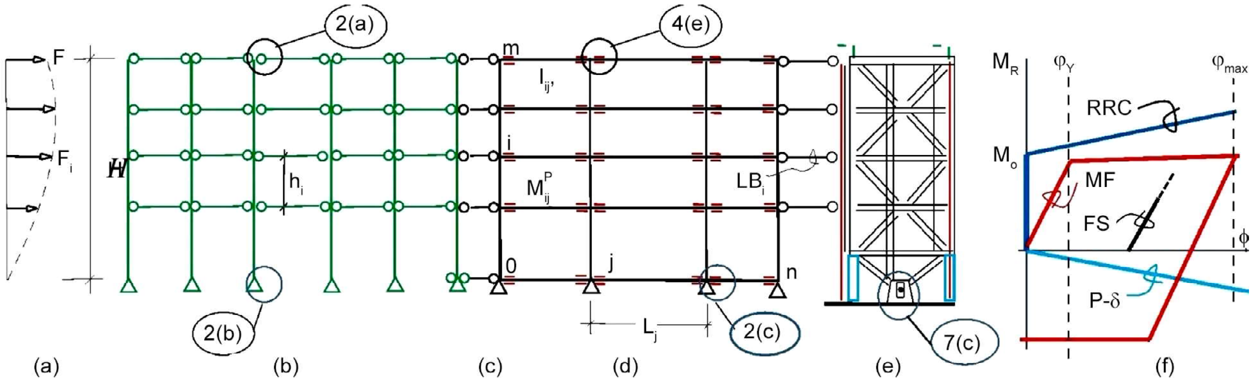

Figure 4. (a) Lateral loading, (b) Special gravity structure, (c) Rigid link beams, (d) seismic sustainability MF with grade beams, (e) Hybrid RRC, and (f) Response diagrams, RRC, MF, FS and Pδ.

the archetype can be estimated as the sum of the two stiffnesses K_F and K_C i.e., $K_S = K_F + K_C$, until one of the two systems reaches first yield. The challenge is to proportion the strengths and stiffnesses of the two structures in such a way as to prevent catastrophic collapse and make it amenable to practical PERR. However, if the M_F is to become a mechanism while the RRC remains perfectly elastic, then the first rule of sequential failures, $(M_F^P / K_F < M_C^P / KC)$, Grigorian and Grigorian (2017), should be satisfied. Although the proposed scheme can be easily analyzed using commercially available software, the authors present a short-cut analytic solution for preliminary design purposes as well as gaining insight into the inner workings of the system. Formula (3) clearly indicates that $\phi = 0$ before the earthquake, endures an Elasto-plastic response during the seismic event as symbolized by Kronecker's deltas $\delta_{i,j}^P$ and $\overline{\delta}_{i,j}^P$ with reduced stiffness $(1-\mu_F)K_F$ and encounters increased stiffness $(1+\mu_F)K_F$ during the recentering process. μ_F is defined in the next section.

4.1. The Elasto-Plastic Analysis of the Multi-Purpose MF

The utility and elegance of the proposed multi-purpose steel MF is not only in its ability to perform as a minimum damage, repairable ERS of uniform drift that lends itself well to PERR, but also the possibility that it can be built as a structure of minimum weight and cost (Brandt, 1978). The basic assumption made here is that the effects of material over-strength, strain hardening, as well as shear and axial strains can be overlooked for all practical purposes. It has also been assumed that the bending effects of small roof and floor loads have little or no direct influence on the side sway and ultimate carrying capacity of the MF (Grigorian and Grigorian, 2012). The high rigidity of the RRC imposes a straight-line drift profile upon the entire system and forces it to act as a function of the same single variable, the drift angle ϕ. In other words, the combination acts as a single degree of freedom (SDOF) system. This implies that the two independent structures and their members all absorb proportional amounts of seismic energies related to the same drift ratios ϕ, regardless of their numbers and locations within the archetype. The implication of this phenomenon is that the elastic force-displacement relationship of the MF of uniform drift, whether by virtue of high-rigidity of a companion structure or purpose specific selection of members of a free-standing frame, can be described in terms of local characteristics of its imaginary horizontal subframes as:

$$\phi_i = \phi = \frac{\left(V_i h_i + M_{P\delta,i}\right)}{12E} + \left[\frac{1}{\sum_{j=0}^{n} \overline{k}_{i,j}} + \frac{1}{2\sum_{i=1}^{n} k'_{i,j}}\right] = \frac{\left(V_i h_i + M_{P\delta,i}\right)}{k'_i} \tag{1}$$

as well as the global properties of its constituent elements (Grigorian & Grigorian, 2011, 2012; Taranath 1998), where $\overline{k}_{i,j} = J_{i,j} / h_i$ and $k'_{i,j} = I'_{i,k} / L_j$. An explanation of use of imaginary horizontal sub-frames is provided in Appendix A. The global static equilibrium of the M_F requires explanation of subframe that

$$M_F = \left(\sum_{i=1}^{m} V_i h_i + M_{P\delta,i}\right) = \sum_{i=1}^{m} K'_i + \phi_i \tag{2}$$

which after some manipulation and rearrangement and introduction of auxiliary symbols gives:

$$\phi = \frac{\left(M_F + M_{P\delta,F}\right)}{12E}\left[\frac{1}{\sum_{i=1}^{m}\sum_{j=0}^{n}\bar{\delta}_{i,j}^{P}\bar{k}_{i,j}} + \frac{1}{\sum_{i=0}^{m}\sum_{j=1}^{n}\delta_{i,j}^{P}k_{i,j}}\right] = \frac{MF}{\left(1 \pm \mu F\right)K_F} \quad (3)$$

where, $k_{i,j} = I_{i,j} / L_{i,j}$, $\bar{k}_{i,j} = J_{i,j} / h_{i,j}$ and $\mu_F = [(K_F / K_S)\sum_{i=1}^{m} P_i h_i = M_{P\delta,F}] / K_F . P_i$ is the total self-weight acting on level i. In general, Kronecker's deltas $\delta_{i,j}^{P}$ and $\bar{\delta}_{i,j}^{P}$ imply structural damage or loss of stiffness with respect to beams and columns *i, j*, respectively and have been introduced to reflect the effects of formation of plastic hinges at prescribed beam locations. By definition, $\delta_{i,j}^{P} = 1$ if $M_{i,j} < M_{i,j}^{P}$, and $\delta_{i,j}^{P} = 0$ if $M_{i,j} = M_{i,j}^{P}$, where, $M_{i,j}$ is the moment acting on the joints of beam *i, j*. $\bar{\delta}_{i,j}^{P} = 0$ implies lack of contribution of column stiffness to global frame stiffness K_F due to the formation of plastic hinges at the ends of the adjoining beams on either side of top and bottom ends of a column. It is instructive to note that as $(M_F + M_{P\delta,F})$ increases, beyond first yield, K_F decreases causing large increases in ϕ, until the M_F is incapacitated. Recentering by GSR and RFA accomplishes the same in the opposite direction, by removing the damaged flange plates and reducing the residual moments to either zero or a minimum until ϕ becomes zero. The use of Rules of sequential failures can improve the efficiency and accuracy of Equation (3) for both the step-by-step response of the MF as well as the GSR+RFA effort. The rule of sequential failures for the MF under consideration states that "While the maximum displacement at incipient collapse is the same as that of the last standing beam or group of beams, the maximum displacement of any intermediate stage is that of the first beam or group of beams, which develops the first set of plastic hinges of that stage" (Grigorian & Grigorian 2012). Because all beams and columns respond simultaneously, the first-stage failure will occur at $\phi_1 = M_{B1}^{P} / K_{B1}$, where ϕ_1 is regarded as the smallest deformation of the loading history of the dual structure. As loading increases, so do the sequential deformations ϕ_r, until a maximum is reached at $j = n$. The progression of the sequential failures can be expressed formally as $\phi_1 + \phi_2 + ... + \phi_j + ...\phi_n$. Since $\phi_{j-1} < \phi_j < \phi_{1j+1}$, it may be concluded that:

$$\frac{M_{B1}^{P}}{K_{B1}} < \frac{M_{B2}^{P}}{K_{B2}} < \frac{M_{B3}^{P}}{K_{B3}} < ... < \frac{M_{Bj}^{P}}{K_{Bj}} < ... < \frac{M_{Bn}^{P}}{K_{Bn}} \quad (4)$$

When using Equations (1) and (4), care should be exercised to relate $M_{col.}$ and $M_{B,j}^{P}$ to point of intersection of the neutral axis and the hinge location, distance a from the column axis, respectively (Figure 3b). The relationship between the two quantities can be expressed as $M_{B,j}^{P} = (1 - (2a_j / L_j))M_{Col.}$.

4.2. Case Study 1- Generation of a MF of Uniform Response

The MF of uniform response of the dual system of Figure (5b) consists of beams of uniform stiffness, where $(L_{i,j} / L_j) = (I_i / L_j)$ and plastic moments of resistance $M_{i,j}^{P} = M_j^{P}$ for each level. Given $\phi_{FS} = \phi_{max}, t_{FS} = t_{flangepl.}$ and $h_i = h$, and the load distribution of Figure (5a), study the effects of activation of the FS plates on the response of the structure. the response plots of the MF, RRC, FS, and P-delta are shown in Figure (5e).

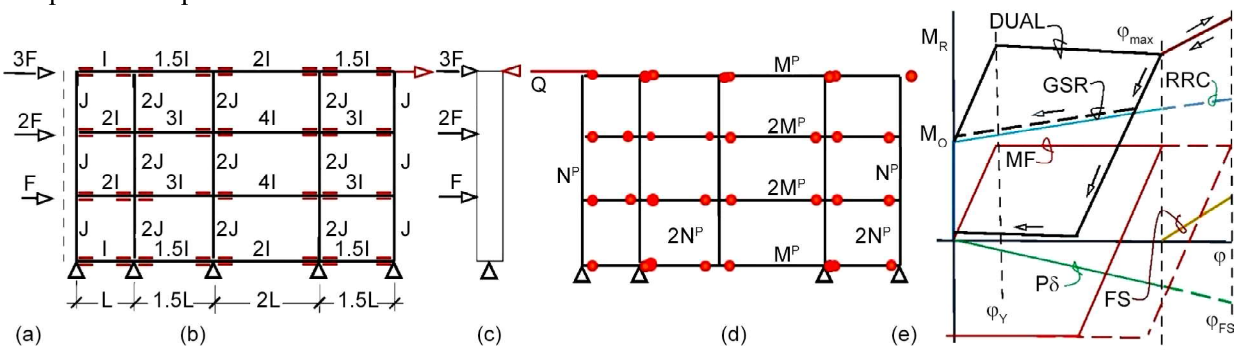

Figure 5. (a) Loading, (b) MF of uniform response, (c) Symbolic RRC, (d) Plastic failure pattern, and (e) Response plot showing the effects of activation of the FS plates and the use of GSR technology.

Due to its high rigidity, the RRC absorbs the entire seismic load and exerts a reaction Q on the MF. The total overturning moment, $M_o = 14Fh$. The roof level interactive reaction $Q = 14Fh / 3\text{h} = 14F/3$. The subframe level shears and racking moments can be computed as $V_3 = V_2 = V_1 = 15\text{F}/3$ and $M_3 = M_2 = M_1 = 14Fh$, respectively. The complete solution to the stiffnesses of the subject MF is presented in Appendix B. Consider the total moment capacity of the three imaginary subframes, each consisting of eight beams of equal plastic moments of resistance $\bar{M}^P_{i,j} = M_i / 4n = M_i = 16$. Thus, $\bar{M}^P_{3,j} = M^P_{2,j} = M^P_{1,j} = (14Fh/3)/16 = 7M^P/24$. Merging the imaginary subframes it gives, $M^P_{3,j} = M^P, M^P_{2,j} = M^P_{1,j} = 2M^P$ and $M^P_{0,j} = M^P$. Consequently, the failure load of the frame may be computed as $M^P_F = 14Fh$. Observing the strong column weak beam principle it gives; $(N^P_{i,0} = N^P_{1,4}) > 2M^P$ and (all other columns) > $4M^P$.

4.3. Case Study 2- Effects of Activation of FS Plates and GSR + RFA

Figure (5e) depicts the individual response diagrams of the RRC, MF, FS, and the $P\delta$ effect in blue, red, green, and brown colors, for $0 \le \phi \le \phi_{max}$, respectively. The underlying assumption here is that non-seismic components neither contribute to seismic resistance nor hinder the PERR process.

The black, flag shape plot represents the combined response of the dual structure before the activation of the FS plates, i.e., when $\phi \le \phi_{max}$. The dashed lines beyond ϕ_{max} display the post-ϕ_{max} responses of the four major components of the system. The short black line on the upper tight hand corner of the diagram illustrates the beneficial effects of the FS plates when the expected design parameters are exceeded. A similar argument can also be presented for the restoring tendons of Figure (3b). The dashed black line to the left of ϕ_{max} shows the recentering path due to GSR and reveals a much smaller flag area, i.e., consumption of restoring energy than that needed for forced realignment. RFA simply means using the built-in stressing jacks and/or turnbuckles to increase or reduce the restoring forces of the supplementary high-strength tendons.

4.4. Case Study 3-Efficiency and Uniform Construction

Both Figures (5b) and (5d) show beams, columns, and connections of uniform construction for all levels with equal bay widths. Uniform construction is one in which all structural items are of the same size and shape regardless of their number and location within their group. Elements of uniform construction lend themselves well to mass production, handling, rapid construction, and realignment. Moreover, the plastic design scheme of Figure (5d) fulfills the requirements of the uniqueness theorem, thereby resulting in a minimum weight solution for the MF under study. Minimum weight and uniform construction together result in the condition known as perfect optimization. In conclusion the proposed SSD can result in highly efficient resilient dual systems.

4.5. Case Study 4-On GSR Scenarios

The use of the proposed dual system becomes even more attractive when the advantages of the GSR technologies are also considered. Figures (5d) indicate that the MF sustains a residual moment of magnitude $M_{Residual} = (14Fh + M_{P\delta})$ on the onset of plastic collapse. The P-delta moment remains affective even after the earthquake and during the PERR process. The force and effort needed to recenter the entire dual system can be considerably reduced by removing some or all the damaged flange plates and FS devices. Several scenarios for the GSR operations and sequences of removal of the moment retaining plates can be envisaged. Assuming $K_C = 0$, the total residual moment without the P-delta effect can be estimated as $(2\times8\,M^P + 2\times8\times2\,M^P) = 48M^P$. A few basic GSR scenario for the subject MF, has been listed in Table (1). Obviously, depending upon the circumstances, many more such scenarios and their combinations can be found. Line 7 indicates that the entire residual moment, except for the P-delta effect can be eliminated. Therefore, the restoring force could be as small as that needed to offset the P-delta moment.

5. The Hybrid Rigid Rocking Core

Regular shear walls and braced frames provide strength and stiffness for dual systems but lack the

Table 1. Basic GSR scenarios for MF of Figure (5) with $K_C = 0$.

Case	Unstiffened Part	P-Delta	Residual Removed	% Reduced
1	Grade Level Beams	$M_{P\delta}$	$-8M^P$	16.7
2	Roof Level Beams	$M_{P\delta}$	$-8M^P$	16.7
3	1st Level Beams	$M_{P\delta}$	$-16M^P$	33.3
4	2nd Level Beams	$M_{P\delta}$	$-16M^P$	33.3
5	Beams of Any Bay	$M_{P\delta}$	$-12M^P$	25.0
6	Beams of Two Bays	$M_{P\delta}$	$-24M^P$	50.0
7	Beams of Three Bays	$M_{P\delta}$	$-36M^P$	75.0
8	Beams of 1 Bay+Level 3,	$M_{P\delta}$	$-24M^P$	50.0
9	Entire Frame	$M_{P\delta}$	$-48M^P$	100

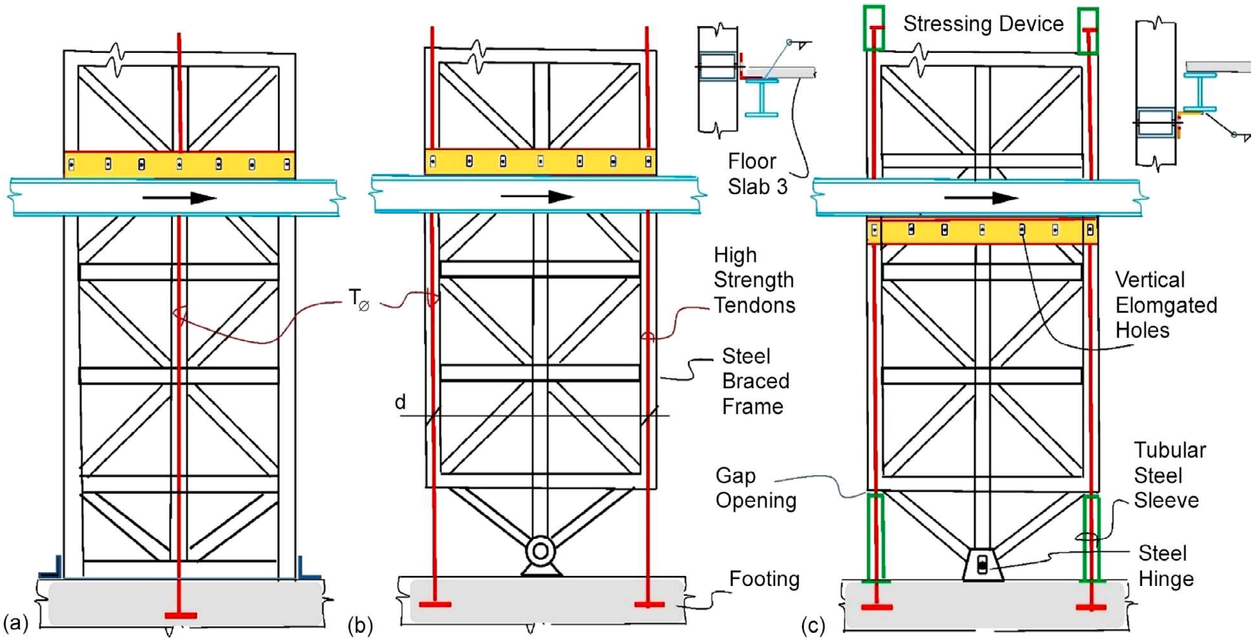

Figure 6. (a) Stepping core, (b) Cable enhanced RRC, and (c) Hybrid RRC with alternative core to floor connection, T_o refers to initial tendon preload.

ability to harvest seismic energies and help realign the combined structure after strong ground shaking, in a regulated and controlled manner. Fixed base shear resisting cores are practically difficult to repair after severe cracking and formation of plastic hinges at their lower ends and restrict the controllability of the entire structure. Almost all shortcomings of fixed base shear cores can be alleviated by introducing centrally hinged supports as shown in Figure (6b). In this respect, the RRC with over 40 favorable attributes (Fahnestock et al., 2021; Grigorian, 2015, 2019, Wada et al., 2012) is remarkable and plays the central role in achieving CP and PERR, it mitigates and precludes several unfavorable conditions that could easily jeopardize the seismic sustainability design. Figures (6a), (6b) and (6c) show schematic views of three types of recently utilized, stepping (FEMA 454, 2006; Deierlein et al., 2009; Chatzis & Smyth, 2012), rocking (Gebelein et al, 2017; Panian et al., 2007), and hybrid (Grigorian et al., 2020), cores, respectively. Both the stepping and the rocking systems have certain merits and drawbacks. Here, the authors propose a novel hybrid rigid rocking-stepping core (Figure 6c) that displays the merits and avoids the drawbacks of both systems. The RRC is considered rigid if its maximum drift ratio does not exceed a fraction of the maximum allowable value, approximately 25%. The new components introduced for the hybrid RRC consist of the built-in stressing jacks, the compression sleeves, and a support-level shear hinge that avoids vertical reaction. The stressing jacks are meant to adjust the twin tendon forces before and after earthquake. The core is initially stressed after resting on top of the sleeves. Depending upon the

Table 2. Comparison of the moment resisting characteristics of the RRCs of Figure 6.

RRC	Rigid Stepping Core		Rigid Rocking Core			Hybrid Rocking Core				
	T_c	M_c	T_l	T_r	M_c	T_l	T_e	M_c	C_l	C_r
At Rest	T_0	--	T_0	T_0	--	T_0	T_0	--	$T_0 + P/2$	
No Gap	$T + T_0$	$(T + T_0 + P)d/2$	$T+T_0$	$T_0 - T$	Td	$T + T_0$	$T_0 - T$	$(T + T_o + P/2)d$	$T_0 - T + P/2$	$T_0 + T + P/2$
Gap	$T + T_o$	$(T + T_0 + P)d/2$	$T+T_0$	0	$(T + T_0)d/2$	$T + T_0$	0	$(T + T_0 + P/2)d$	0	$T_0 + T + P/2$
Opng	$T \geq (T_0 + P)$		$T \geq T_0$			$T \geq (T_0 + P/2)$				

type of construction, diaphragm shears can be transferred to the RRC through un-bonded stressed tendons, link beams and buckling restrained braces.

In either case, damage to the core-slab interface should be avoided by releasing the vertical components of the continuous bolted connection. The physical clearance between the slabs and the RRC and the vertically elongated bolt holes prevent the core-slab connections from being damaged during earthquakes, allow free movement of the core, and provide out-of-plane stability for the RRC. The restoring characteristics of RRCs are defined by their rigidity, ultimate strength, and base level rotational stiffness. The sleeves can also be designed as primary or backup FS devices.

5.1. Case Study 5- Compare the Resistance of the Three RRCs of Figure (6)

A complete summary of this study is presented in Table (2), where letters T and C stand for cable tension and sleeve compression, respectively, and subscripts l and r refer to left- and right-hand sides, respectively, which shows that the main advantage of the hybrid system over the stepping core is that the moment resisting lever arm of the former is twice that of the latter. Meanwhile, utilization of the sleeves eliminates the loss of pretension in the leeward tendons. The sleeves also provide static stability for the RRC and act as fail-safe devices against tendon snapping and relaxation. Note that the sleeves and tendons are treated as compression and tension only members, respectively.

The core drift ratio can be expressed in terms of core moment M_C and rotational stiffness K_C as:

$$\phi = \left[\frac{H}{A_t E_t} + \frac{h}{A_s E_s}\right]\frac{M_c}{d^2} = \frac{M_c}{K_c} \tag{5}$$

Here, A and E define section area and young's modulus, respectively, and subscripts t and s stand for tendon and sleeve, respectively. H and h refer to effective tendon length and sleeve height, respectively. K_C=0 if neither the high strength tendons nor steel sleeves are used as supplementary elements.

6. Conclusions

The paper presents a framework for development of seismic sustainability with a view to efficient design of dual steel structures. The efforts leading to the preparation of this article were prompted by the need to promote SSD for resilient cities and the suggestions made by the researchers cited in this paper. The main purpose of the current contribution is to encourage engineers to look at integration of sustainability in their designs as a moral obligation rather than entertaining an abstract idea. The philosophy is relatively new and needs the test of time and professional support before it is publicly recognized as an important social issue. SSD, is a relatively new trend of thought that is being discussed within structural engineering communities worldwide. SSD is inclined towards long term, environmental welfare rather than short-lived, client-based standards for performance. The introduction of SSD is proceeded by development of components of a novel seismic sustainability dual steel archetype. The research effort leading to the preparation of this paper was prompted by the notion that SS design can be achieved in accordance with the following practical issues in mind, that:

- The structure is an SDOF system. Within the constraints of the theoretical presumptions, a half-cycle precise analysis has been developed using straightforward closed-form solutions.
- Fail-safe technologies are devised to reduce and/or prevent damage due to premature activation of failure mechanisms. For this case,

the FS devices can be used to activate the post-yield reserve capacities of the structure for CP and PERR. FS technologies are indispensable parts of SSD of engineering structures.

- Uniform construction is one in which all structural items such as beams, columns, braces, connections, and joints are of the same size and shape, regardless of their number and location, within their group. Such items lend themselves well to mass production, handling, rapid construction, and realignment. MFs of uniform construction also fulfill the requirements of the uniqueness theorem, and result in minimum weight solutions. In conclusion, the proposed SSD can result in highly efficient resilient dual/multiple systems.
- Two recently-developed technologies, GSR and RFA, which reduce and/or modify the strength of the restoring forces required to realign the structure, can be used to achieve recentering.
- All of the rocking core-moment frames mentioned in this article have passed time history analysis and experimentation testing. Extensive computer analysis supports the viability of the parametric cases presented in this paper.
- The suggested structural plans are still in their early stages. They still need to be refined and put to the test in order to become practical, earthquake-resistant systems.

The authors hope this article will help promote the development of future building codes and college curricula for the design of seismically sustainable structures.

References

Akbari, A., Massumi, A., & Grigorian, M. (2023). Seismic performance evaluation of steel moment frames with mid-span rigid rocking cores. *Steel and Composite Structures*, *46*(5), 621-640. https://doi.org/10.12989/scs.2023.46.5.621

Ajrab, J., Pekcan, G., & Mander, J. B. (2004). Rocking wall-frame structures with supplemental tendon systems. *Journal of Structural Engineering*, *130*(6), 895-903.

Astaneh-Asl, A. (1997). Seismic design of steel column-tree moment-resisting frames. *Structural Steel Educational Council*.

Astaneh-Asl, A., Call, S. M., & McMullin, K. M. (1989). Design of single plate shear connections. *Engineering Journal*, *26*(2), 21-31.

American Society of Civil Engineers. (2016). *Minimum Design Loads and Associated Criteria for Buildings and Other Structures (ASCE/SEI 7-16)*. ASCE.

Ansari Targhi, R., Ansari Targhi, M., Grigorian, M., & Boroujerdian, V. (2024). Development of sustainable seismic structures. In *Proceedings of the 9th International Conference on Seismology and Earthquake Engineering*, Tehran, Iran.

Brandt, A. (1978). *Criteria and Methods of Structural Optimization*. Kluwer Academic Publishers.

Beedle, L. S. (1985). *Plastic Design of Steel Frames*. John Wiley & Sons.

Bozkurt, M. B., & Topkaya, C. (2018). Replaceable links with gusseted brace joints for eccentrically braced frames. *Soil Dynamics and Earthquake Engineering*, *115*, 305-318.

Chancellor, N. B., Eatherton, M. R., Roke, D. A., & Akbas, T. (2014). Self-centering seismic force-resisting systems: High-performance structures for the city of tomorrow. *Buildings*, *4*(3), 520-548.

Chatzis, M. N., & Smyth, A. W. (2012). Modeling of the 3D rocking problem. *International Journal of Non-Linear Mechanics*, *47*(4), 85-98.

Deierlein, G. G., Ma, X., & Eatherton, M. R. (2009). Collaborative research on development of innovative steel braced frame systems with controlled rocking and replaceable fuses. In *Proceedings of the 6th International Conference on Urban Earthquake Engineering*, 413-416.

Dowden, D. M., & Bruneau, M. (2011). Steel and Composite. *Structures*, *48*, 153-166.

European Committee for Standardization. (1998). *Eurocode 8: Design of Structures for Earthquake Resistance*.

Eatherton, M. R., Ma, X., Krawinkler, H., Deierlein, G. G., & Hajjar, J. F. (2014). Quasi-static cyclic behavior of controlled rocking steel frames. *Journal of Structural Engineering*, *140*(11), 04014083.

Foulkes, J. (1953). Minimum weight design and the theory of plastic collapse. *Quarterly of Applied Mathematics*.

Fahnestock, L., Sause, R., Ricles, J., Simpson, B., Kurata, M., Okazaki, T., Kawamata, Y., Tao, Z., Duke, J., Rivera, D., Astudillo, B., & Qie, Y. (2021). U.S.-Japan collaboration for shake table testing of a frame-spine system with force-limiting connections. In *Proceedings of the 17th World Conference on Earthquake Engineering (17WCEE)*.

Federal Emergency Management Agency. (2006). *FEMA 454: Designing for earthquakes: A manual for architects. FEMA*.

Gebelein, J., Barnard, M., Burton, H., et al. (2017). Considerations for a framework of resilient structural design for earthquakes. In *Proceedings of the SEAOC Convention*.

Gilmore, A. T. (2012). Options for sustainable earthquake-resistant design of concrete and steel buildings. *Earthquakes and Structures*, *3*(6), 783-804.

Grigorian, M., & Grigorian, C. (2011). Performance control for seismic design of moment frames. *Journal of Constructional Steel Research*, *67*(7), 1106-1114.

Grigorian, M., & Grigorian, C. (2012). Performance control: A new elastic-plastic design procedure for earthquake-resisting moment frames. *Journal of Structural Engineering*, *138*, 473-483.

Grigorian, M. (2014a). Biomimicry and theory of structures: Design methodology transfer from trees to moment frames. *Journal of Bionic Engineering*, *11*(4).

Grigorian, M. (2014b). Performance control based on green tree behavior. *Asian Journal of Civil Engineering*, *15*(6), 897-922.

Grigorian, M., & Grigorian, C. (2015). *An Introduction to the Structural Design of Rocking Wall-Frames with a View to Collapse Prevention, Self-Alignment and Repairability*. The Structural Design of Tall and Special Buildings.

Grigorian, M., & Grigorian, C. (2017). Sustainable earthquake-resisting system. *Journal of Structural Engineering*, *144*(2), 04017199.

Grigorian, M., & Kamizi, M. (2019a). *On the Analysis of Multilevel Rocking Cores: A Bioinspired Analogy. Engineering Reports*. https://doi.org/10.1002/eng2.12025

Grigorian, M., Moghadam, A. S., & Kamizi, M. (2019b). On repairable earthquake-resisting archetypes with a view to resiliency objectives and assisted self-centering. *The Structural Design of Tall and Special Buildings*, e1603. https://doi.org/10.1002/tal.1603

Grigorian, M., & Kamizi, M. (2019c). High-performance resilient earthquake-resisting moment frames. *Proceedings of the Institution of Civil Engineers: Structures and Buildings*. https://doi.org/10.1680/jstbu.19.00109

Grigorian, M., Kamizi, M., & Sedighi, S. (2020). A basis for developing sustainable earthquake-resisting structures. *Proceedings of the Institution of Civil Engineers: Structures and Buildings*. https://doi.org/10.1680/jstbu.20.00053

Grigorian, M., Moghadam, A. S., & Sedighi, S. (2022). Sustainable seismic design and health monitoring. *Structural Control and Health Monitoring*, *29*(11), e3058. https://doi.org/10.1002/stc.3058

Grigorian, M., Sedighi, S., Ansari Targhi, M., & Ansari Targhi, R. (2023). Sustainable earthquake-resistant mixed multiple systems. *Journal of Structural Engineering*. https://doi.org/10.1061/JSENDH/STENG-11510

Gunay, S., & Mosalam, K. M. (2013). PEER performance-based earthquake engineering methodology revisited. *Journal of Earthquake Engineering*, 17(6), 829-858.

Heyman, J. (1971). *Plastic Design of Frames*. Cambridge University Press.

Hajjar, J. F., Sesen, H., Jampole, E., & Wetherbee, A. (2013). *A Synopsis of Sustainable Structural Systems with Rocking, Self-Centering, and Articulated Energy-Dissipating Fuses (Report No. NEU-CEE-2013-01)*. Northeastern University.

IACGE. (2018). Seismic research and practices for sustainability. *Proceedings of the International*

Conference on Geotechnical and Earthquake Engineering.

Janhunen, B., Tipping, S., Wolfe, J., & Mar, D. (2012). Seismic retrofit of a 1960s steel moment-frame high-rise using a pivoting spine. In *Proceedings of the Annual Meeting of the Los Angeles Tall Buildings Structural Design Council*.

Kam, W. Y., & Jury, R. (2015). Performance-based seismic assessment: Myths and fallacies. In *Proceedings of the NZSEE Conference*, 673-687.

Karavasilis, T. L., Blakeborough, A., & Williams, M. S. (2011). Development of nonlinear analytical model and seismic analyses of a steel frame with self-centering devices and viscoelastic dampers. *Computers & Structures*, *89*(11-12), 1232-1240.

Lu, Y., & Panagiotou, M. (2014). Earthquake damage-resistant multistory buildings using combination of base isolation and rocking core walls. In *Proceedings of the 1st Huixian International Forum on Earthquake Engineering*.

MacRae, G., Kimura, Y., & Roeder, C. (2004). Effect of column stiffness on braced frame seismic behavior. *Journal of Structural Engineering*, *130*, 381-391.

Ma, X., Borchers, E., & Pena, A. (2011). *Design and behavior of Steel Shear Plates with Openings as Energy Dissipating Fuses (Technical Report No. 173)*. John A. Blume Earthquake Engineering Center, Stanford University.

Mahin, S. A. (2017). Resilience by design: A structural engineering perspective. In *Proceedings of the 16th World Conference on Earthquake Engineering (16WCEE)*, Santiago, Chile.

Neal, B. G. (1963). *The Plastic Methods of Structural Analysis*. Chapman & Hall.

Naeim, F. (2001). *The Seismic Design Handbook*. Kluwer Academic Publishers.

Pampanin, S. (2015). Towards the "ultimate earthquake-proof" building: Development of an integrated low-damage system. In A. Ansal (Ed.), *Perspectives on European Earthquake Engineering and Seismology*, 7-16. Springer. https://doi.org/10.1007/978-3-319-16964-4_2

Panian, L., Steyer, M., & Tipping, S. (2007). An innovative approach to earthquake safety and concrete construction. *Journal of the Post-Tensioning Institute*, *5*, 7-16.

Pessiki, S. (2017). Sustainable seismic design. *Procedia Engineering*, *171*, 33-43.

Pollino, M., Slovenec, D., Qu, B., & Mosqueda, G. (2017). Seismic rehabilitation of concentrically braced frames using stiff rocking core. *Journal of Structural Engineering*, *143*(9). https://doi.org/10.1061/(ASCE)ST.1943-541X.0001810

Priestley, M. J. N., & Kowalsky, M. J. (2000). Direct displacement-based seismic design of concrete buildings. *Bulletin of the New Zealand Society for Earthquake Engineering*, *33*(4), 421-444.

Richards, R. H., Gillett, P. E., Kriegh, J., & Lewis, B. A. (1980). The analysis and design of single plate framing connections. *Engineering Journal*, *17*(1).

Spencer, B. F., Jr., & Nagarajaiah, S. (2003). State of the art of structural control. *Journal of Structural Engineering*, *129*(7), 845-856. https://doi. org/10.1061/(ASCE)0733-9445(2003)129:7(845)

Takagi, J., & Wada, A. (2019). Recent earthquakes and the need for a new philosophy for earthquake-resistant design. *Soil Dynamics and Earthquake Engineering*, *119*, 499-507. https://doi.org/10.1016/j.soildyn.2019.01.017

Taranath, B. S. (1998). *Steel, Concrete and Composite Design of Tall Buildings*. McGraw-Hill.

International Conference of Building Officials. (1992). *Uniform Building Code (UBC). Author*.

Wada, A., & Mori, N. (2008). Seismic design for the sustainable city: A report on Japanese practice. In *Proceedings of the ASCE Structures Congress*. https://doi.org/10.1061/41016(314)123

Wada, A., Qu, Z., Ito, H., et al. (2012). Pin-supported walls for enhancing the seismic behavior of building structures. *Earthquake Engineering & Structural Dynamics*, *41*(14), 2075-2091.

Wang, J., & Hua, Z. (2018). High-performance damage-resistant seismic-resistant structural

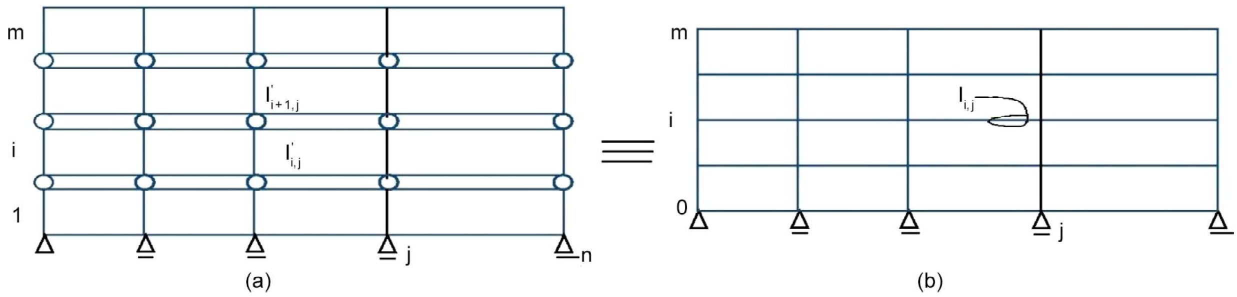

Figure A1. (a) Hypothetical subframes and (b) Original frame.

systems for sustainable and resilient cities: A review. *Shock and Vibration*, Article 8703697. https://doi.org/10.1155/2018/8703697

Wiebe, L., & Christopoulos, C. (2014). Controlled rocking systems for enhanced seismic resilience: State of the art. In X. Liu & A. H.-S. Ang (Eds.), Sustainable development of critical infrastructure, 496-503. ASCE.

Yao, J. T. P. (1972). Concept of structural control. *Journal of the Structural Division*, *98*(7), 1567-1574.

Appendix A

The use of imaginary horizontal subframes helps achieve exact short-cut solution for determination of the unknown interactive forces between the MF and the RRC. The partial sketch of a generalized MF of uniform drift together with its imaginary horizontal subframes connected to each other by means of hypothetical rigid links is shown in Figure (A1).

These subframes are forced to deform compatibly and to remain in static equilibrium throughout the loading history of the structure. Clearly, when the imaginary subframes are merged to reassemble the original frame, the hypothetical links disappear and the moments of inertia and bending moments of the beams and columns of the reconstructed structure become $I_{i,j} = I'_{i,j} + I'_{i+1,j}$, $J'_{i,j} = J_{i,j}$ and $M_{B,i,j} = M'_{B,i,j} + M'_{B,i+1,j}, M'_{C,i,j} = M_{ci,j}$ respect-tively, with the exce-ption of the roof and grade-level beams for which the moments of inertia may be expressed as $I_{m,j} = I'_{m,j}$ and $I_{0,j} = I'_{0,j}$ respectively. And if needed, the sum of the plastic moment of resistance of the merging beams of two consecutive subframes becomes $M^P_{B,i,j} = M'^P_{B,i,j} + M'^P_{B,i+1,j}$.

Appendix B

The rule of constant stiffness for the upper level beams of the 3rd level subframe requires that $I_{3,1} = I(L_1 / L_1) = I$, $I_{3,2} = I(1.5L / L) = 1.5I$, $I_{3,3} = I(2L / L) = 2I$ and $I_{3,4} = I(1.5L / L) = 1.5I$.

The rule of proportionality for the stiffnesses of the beams of the MF of uniform drift requires that; $I_{i,j} = \overline{I}_{i,j} + \overline{I}_{i+1,j}$ where $\overline{I}_{i,j} = \overline{I}_{m,j}(M_i / M_m)$. Similarly, the rule of proportionality for the stiffnesses of the columns requires that $J_{i,0} = J_{i,n} = J_{m,0}(M_i / M_m)$ and $J_{i,1} = J_{i,2} ..... = J_{i,n-1} = 2J_{i,0}$.